ISSN 0023-1584, Kinetics and Catalysis, 2006, Vol. 47, No. 2, pp. 160–169. © MAIK "Nauka/Interperiodica" (Russia), 2006.

Kinetic and Mechanism of Alkene Polymerization[1]

M. Bochmann, R. D. Cannon, and F. Song

Wolfson Materials and Catalysis Centre, School of Chemical Sciences and Pharmacy, University of East Anglia, Norwich NR4 7TJ, UK
e-mail: m.bochmann@ula.ac.uk

Received July 11, 2005

Abstract—Triphenylmethyl salts of the very weakly-coordinating borate anions $[CN\{B(C_6F_5)_3\}_2]^-$ (**1**), $[H_2N\{B(C_6F_5)_3\}_2]^-$ and $[M\{CNB(C_6F_5)_3\}_4]^{2-}$ (M = Ni, Pd) have been prepared in simple one-pot reactions. Mixtures of (SBI)$ZrMe_2$/**1**/$AlBu^i_3$ (SBI = *rac*-$Me_2Si(Ind)_2$) are 30–40 times more active in ethylene polymerizations at 60–100°C than (SBI)$ZrCl_2$/MAO. The quantification of anion effects on propene polymerization activity at 20°C gives the order $[CN\{B(C_6F_5)_3\}_2]^- > [H_2N\{B(C_6F_5)_3\}_2]^- \approx B(C_6F_5)^-_4 \gg [MeB(C_6F_5)_3]^-$. The highest productivities were of the order of ca. 3.0×10^8 g PP (mol Zr)$^{-1}$ h^{-1} $[C_3H_6]^{-1}$, about 1.3–1.5 times higher than with $B(C_6F_5)^-_4$ as the counter anion. The titanium system $CGCTiMe_2$/**1**/$AlBu^i_3$ gave activities that were very similar to the zirconocene catalyst. The concentration of active species [C*] as determined by quenched-flow kinetic techniques indicates typical values of around 10%, independent of the counter anion, for both the borate and MAO systems. Pulsed field-gradient spin echo and nuclear Overhauser effect NMR experiments on systems designed to be more realistic models for active species with longer polymeryl chains, (SBI)$M(CH_2SiMe_3)(\mu$-$Me)B(C_6F_5)_3$ and $[(SBI)MCH_2SiMe^+_3 \cdots B(C_6F_5)^-_4]$ (M = Zr, Hf), demonstrated the influence of bulky alkyl chains on the ion pair solution structures: while the $MeB(C_6F_5)_3$ compound exists as a simple inner-sphere ion-pair, the $B(C_6F_5)^-_4$ compound is an outer-sphere ion pair (OSIP), a consequence of the relegation of the anion into the second coordination sphere by the γ-agostic interaction with the alkyl ligand. The OSIP aggregates to ion hextuples (10 mM) or quadruples (2 mM). Implications for the polymerization mechanism are discussed; the process follows an associative interchange (I_a) pathway.

DOI: 10.1134/S0023158406020029

Highly electrophilic metallocene cations paired with non-nucleophilic, very weakly coordinating anions are known to be highly active catalysts for the Ziegler-type polymerization of olefins (Scheme 1) [1–5]. For the effective binding of substrates as weakly basic as alkenes, a strongly Lewis acidic metal centre is required. This Lewis acidity is controlled by the nature of the counter anion, and it is therefore not surprising that significant efforts have been invested in the way of anion engineering [6, 7]. A few pertinent examples are shown in Scheme 2. Of these, $B(C_6F_5)^-_4$ and the methylborate $MeB(C_6F_5)^-_3$ derived from $B(C_6F_5)_3$ are the most widely used, while other examples are synthetically less accessible [8–38].

RESULTS AND DISCUSSION

Anion synthesis. We are interested in methods of generating new bulky anions in a more straightforward manner. The overriding principle for this anion design is the desire to delocalize the negative charge over as large a volume as possible. This can be achieved, for example, by the facile adduct formation between commercially available $B(C_6F_5)_3$ and strongly coordinating anions such as CN^-. For example, stirring a suspension of KCN with two equivalents of $B(C_6F_5)_3 \cdot Et_2O$ in diethyl ether at room temperature followed by treatment with Ph_3CCl gives $[CPh_3][CN\{B(C_6F_5)_3\}_2]$ (**1**) as orange crystals. The linear CN-bridged geometry of **1**

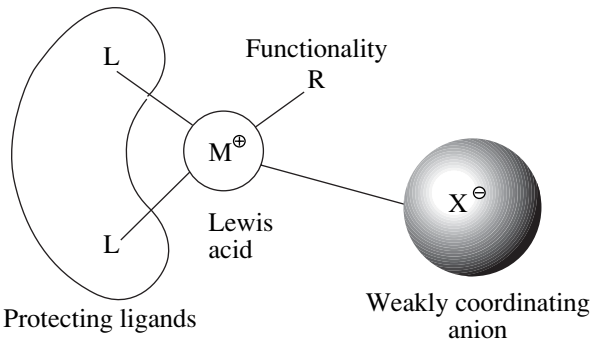

Scheme 1.

[1] The text was submitted by the authors in English.

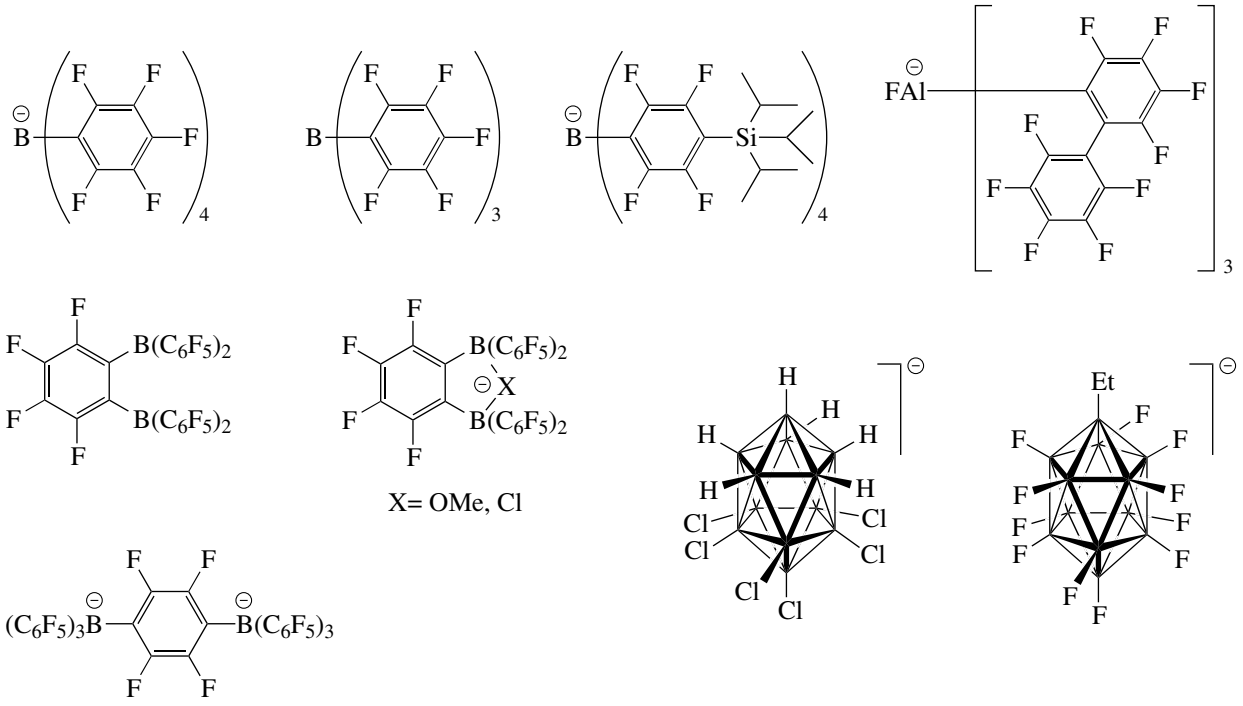

Scheme 2. Representative examples of weakly coordinating anions.

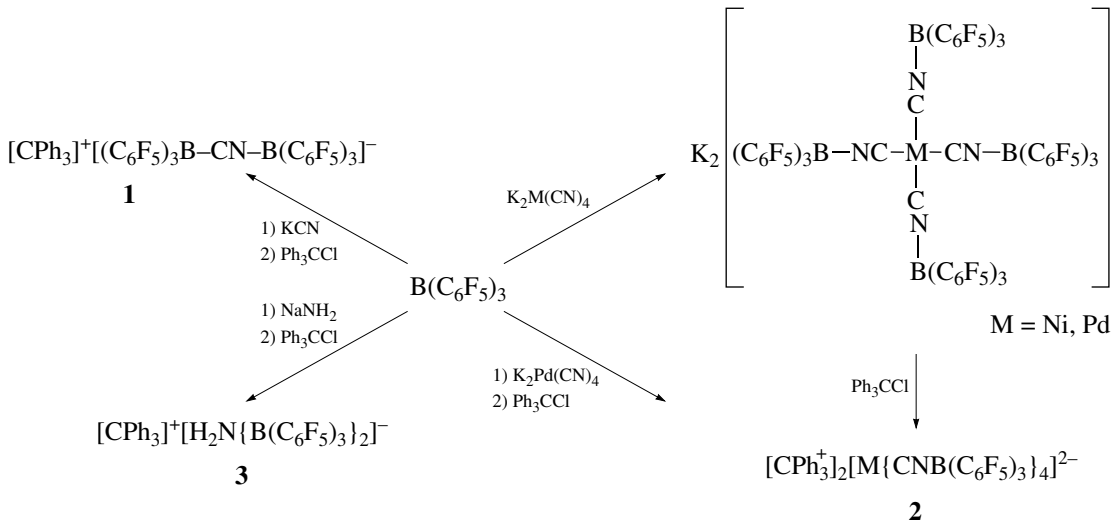

Scheme 3.

was confirmed by X-ray crystallography, the ν_{CN} stretching frequency at 2305 cm^{-1}, and the observation of two ^{11}B NMR signals at δ –11.94 and –21 [39, 40]. A similar reaction between $B(C_6F_5)_3 \cdot Et_2O$ and the very stable nickel and palladium tetracyanometallates $[M(CN)_4]^{2-}$ leads to the dianions $[M\{CNB(C_6F_5)_3\}_4]^{2-}$ (**2**, M = Ni, Pd), which were isolated as $NHMe_2Ph^+$ and CPh_3^+ salts (Scheme 3) [41].

Similarly, the reaction of $NaNH_2$ with two equivalents of $B(C_6F_5)_3$ gives $[Na(OEt_2)_4][H_2N\{B(C_6F_5)_3\}_2]$, which is readily converted into the trityl salt $[CPh_3][H_2N\{B(C_6F_5)_3\}_2]$ (**3**); the whole process can conveniently be conducted as a one-pot reaction [42, 43]. As the crystal structure of this anion shows, it is significantly stabilized by NH···F hydrogen bonds to five ortho-F atoms (Fig. 1). The resistance of the diborate anion towards protolysis is illustrated by the conversion

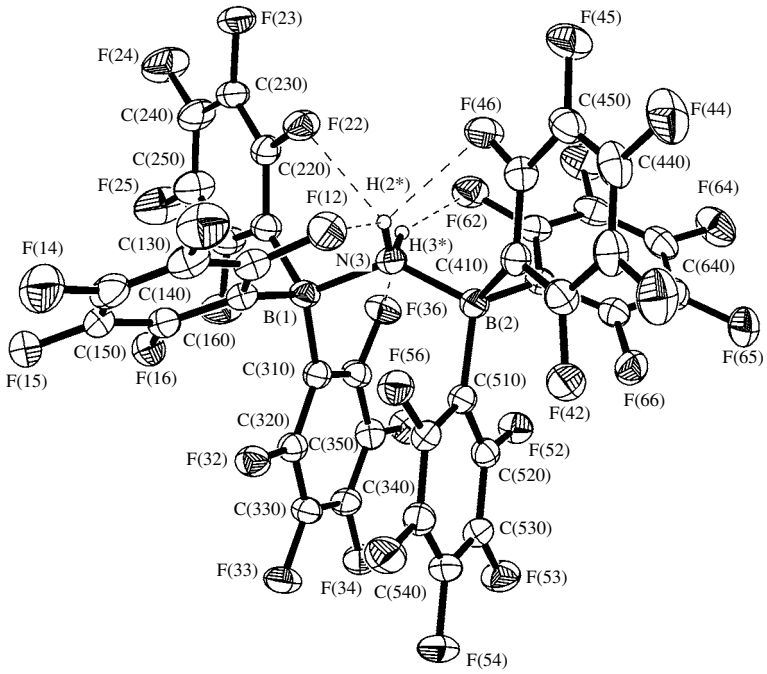

Fig. 1. Structure of the anion $[H_2N\{B(C_6F_5)_3\}_2]^-$ in the solid state, illustrating the H···F hydrogen bonding to five of the six *o*-F atoms.

of the sodium salt into crystalline $[H(OEt_2)_2][H_2N\{B(C_6F_5)_3\}_2]$. The formation of this strong Brønsted acid is favored over protolytic anion decomposition, e.g., to give $H_3N \cdot B(C_6F_5)_3 + Et_2O \cdot B(C_6F_5)_3$.

Quantification of anion effects. Our interest in new catalyst activators based on complex borate anions was not least kindled by our observation that the ethylene polymerization activity of a standard catalyst like (SBI)$ZrMe_2$ (SBI = *rac*-$Me_2Si(Ind)_2$) was increased by a factor of 30–40 if a mixture of $AlBu^i_3$ (TIBA) and **1** was used as the activator instead of methylaluminoxane (MAO) [39, 40]. In effect, the activity (productivity) of a catalyst is one of the most difficult parameters to quantify objectively. This is perhaps best illustrated by Möhring and Coville's compilation of literature data for the activity of the "standard" ethene polymerization catalyst Cp_2ZrCl_2/MAO, which cover a range of four orders of magnitude [44]. In order to compare anion effects with metallocene catalysts, we have developed a protocol that eliminates concentration and mass transport effects. To reduce the problem of monomer depletion in reactions under 1 bar monomer pressure, propene rather than ethylene polymerization was investigated. The results show that at 20°C catalyst productivity decreases in the order $[CN\{B(C_6F_5)_3\}_2]^- > [H_2N\{B(C_6F_5)_3\}_2]^- \approx B(C_6F_5)_4^- \gg [MeB(C_6F_5)_3]^-$. With (SBI)$ZrMe_2$/**1**/$AlBu^i_3$ and [Zr] = 5×10^{-6} mol/L, productivities were of the order of ca. $(2.8–3.0) \times 10^8$ g PP (mol Zr)$^{-1}$ h^{-1} $[C_3H_6]^{-1}$, about 1.3–1.5 times higher than with $B(C_6F_5)_4^-$ as the counter anion. The titanium system CGCTiMe_2/**1**/$AlBu^i_3$ gave activities that were very similar to the zirconocene catalyst. The almost linear dependence of catalyst activity on [Zr] makes it possible to extrapolate to zero catalyst concentration in order

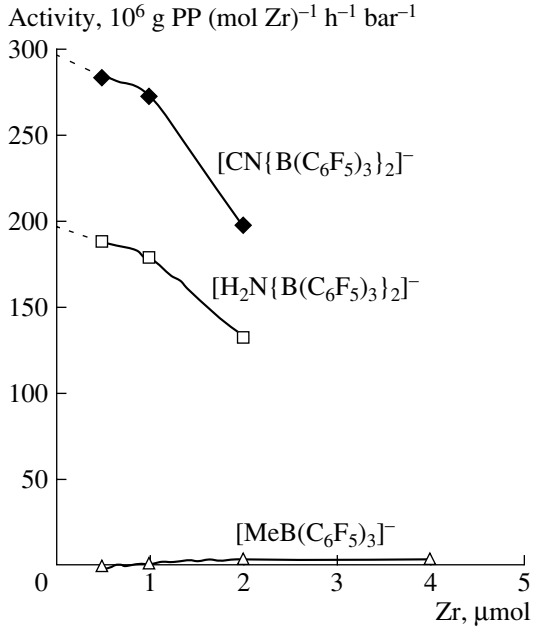

Fig. 2. Dependence of propene polymerization activity on [Zr].

to determine the "intrinsic" activity of the system (Fig. 2) [41].

Polymerization kinetics. The classical picture of the mode of action of metallocene-based catalysts assumed dissociation into an ion pair, with the cationic metallocenium alkyl species being responsible for chain propagation, while the anion was not thought to be involved (Scheme 4) [3, 4]. However, the fact that the anion does contribute to the activation barrier of polymerization must mean that it is involved in the transition state. The question therefore was whether the anion-dependent differences in activity were due to differences in the concentration of active species [C*] or to the lowering of the transition state.

This problem was probed using quenched-flow kinetic techniques [45–49]. Two catalyst systems were used: (a) (SBI)$ZrMe_2$/TIBA/$CPh_3[CN\{B(C_6F_5)_3\}_2]$ and (b) (SBI)$ZrCl_2$/MAO, both at 1 bar propene in toluene. This system allowed us to investigate the onset of polymerization under homogeneous, as opposed to mass-transport limited conditions, from t_R = 0.2 to 5 s [50–52].

The results provide two independent types of data. The time dependence of polymer mass assumes that 100% of the injected pre-catalyst was active and leads to the "apparent" propagation rate constant, k_p^{app}. The second source of data is the time dependence of the number-average polymer molecular weight, which makes no assumptions about the concentration of active species. From this a second rate constant k_p was obtained for the rate of growth of the polymer chains. The ratio k_p^{app}/k_p is therefore a measure of the proportion of total zirconocene that is active at any one time. Of course (neglecting irreversible deactivation), due to ligand redistribution most of the injected zirconocene will be involved in the chain growth process over time and will carry a polymeryl chain. Measurements of [C*] by isotopic labelling techniques will therefore

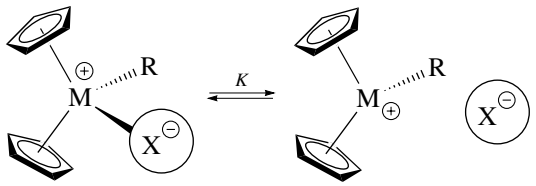

Scheme 4.

result in values that approach 100%. On the other hand, the [C*] values determined by quenched-flow kinetics were much smaller, 8%. Surprisingly, this value was the same for both the borate and the MAO-activated system. It follows that there must be a distribution between active and dormant species that is the same for both catalyst systems, as well as that the MAO-catalyst takes significantly longer to complete one insertion cycle. Other systems, such as the CGCTi catalysts, show similar [C*] (table) [45, 49].

Further information about the possible nature of the dormant sites comes from the polymer microstructure and end group analysis [53, 54]. Both vinylidene and *cis*-butenyl (vinylene) end groups are found, the latter being dominant in this system. There is also a contribution from internal C=C bonds, which are a follow-on product of vinylidene end groups. Taking this into account gives a vinylidene : butenyl ratio of 34 : 66. There is a small number of enchained regioerrors due to 2,1-insertions followed by 1,2-chain growth, on average one per 500 1,2-insertions (Scheme 5). Since most of the end groups are generated following a 2,1-misinsertion, and since termination reactions in polymerization systems are orders of magnitude slower than propagation reactions, it is clear that a substantial amount of total [Zr] must be present as Zr-*sec*-alkyl species; these, therefore, make an important contribution to the total resting states in this system.

The mechanistic scheme we used to rationalize our findings and the relevant rate constants for propagation

Proportion of active species in propene polymerizations with various metallocene catalysts

Catalyst	k_p^{app} (yield vs. time), l mol^{-1} s^{-1}	k_p (M_n vs time), l mol^{-1} s^{-1}	Fraction of active species, k_p^{app}/k_p
(SBI)$ZrMe_2$/TIBA/$CPh_3[CN\{B(C_6F_5)_3\}_2]$	1320 ± 20	17200 ± 1400	0.08
(SBI)$ZrCl_2$/MAO	48 ± 3	600 ± 230	0.08
(SBI)$ZrCl_2$/TIBA/$CPh_3[B(C_6F_5)_4]$ (1 : 100 : 1)	1100	8800	0.13
(SBI)$ZrCl_2$/TIBA/$CPh_3[B(C_6F_5)_4]$ (1 : 100 : 3)	2500	11200	0.22
(CGC)$TiMe_2$/TIBA/$CPh_3[B(C_6F_5)_4]$	1100	7400	0.15
(CGC)$TiCl_2$/TIBA/$CPh_3[B(C_6F_5)_4]$	2800	19300	0.15

Note: Toluene, $[C_3H_6]$ = 0.6 M, 25°C.

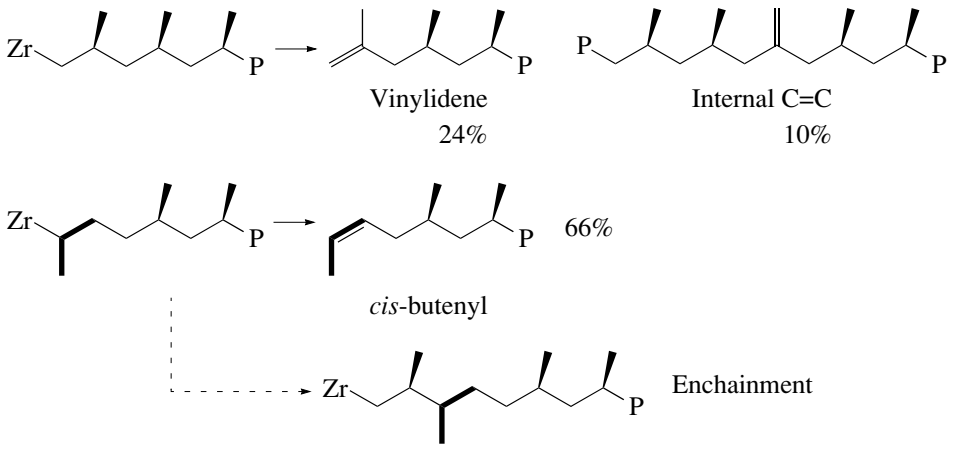

Scheme 5.

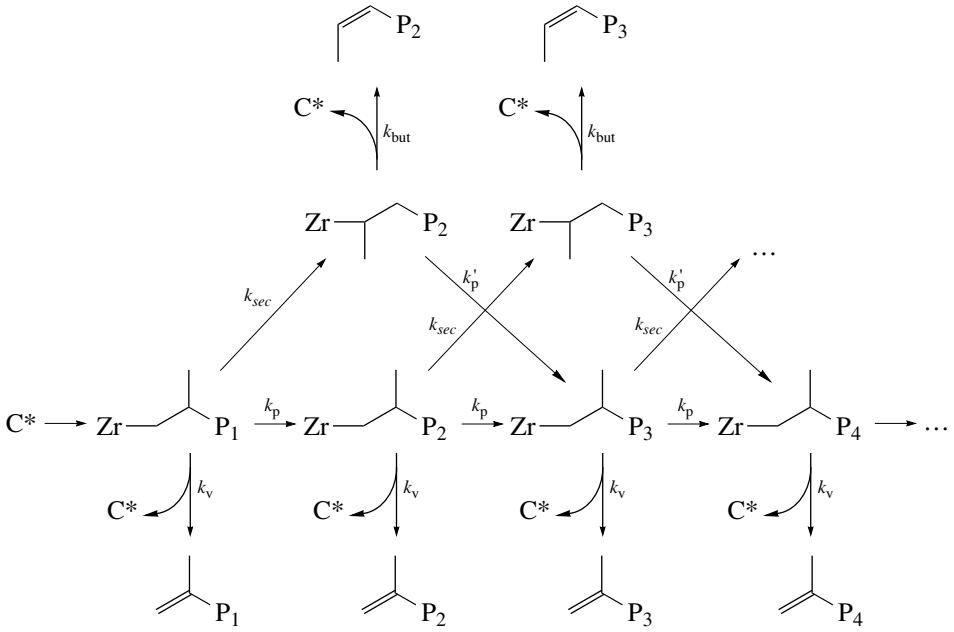

Scheme 6.

and termination processes is depicted in Scheme 6 [45]. Some doubt has been raised in the literature as to the existence of dormant states, and the accumulation of *sec*-alkyl zirconocene species in particular, based on spectroscopic studies of the (EBI)$ZrMe_2/B(C_6F_5)_3$ system (EBI = *rac*-C_2H_4(1-Ind)$_2$), which indeed leads almost exclusively to vinylidene end groups [55, 56]. However, based on a combination of kinetic results and the polymer microstructure analysis, we estimate the lifetimes of the primary and secondary alkyls to be τ(Zr-*Prim*) = $1/(k_p + k_{sec})[M] \approx 10^{-4}$ s, and τ(Zr-*Sec*) = $1/(k_p' + k_{but})[M] \approx 10^{-1}$ s, respectively; in other words, the data suggest that under catalytic conditions a *sec*-alkyl zirconocene species persists ca. 10^3 times longer than a *prim*-alkyl species, long enough to accumulate as a dormant state.

Inner-sphere versus outer-sphere ion pairs. The catalyst systems employed so far have been based on zirconocene dimethyls or dichlorides in combination with TIBA and an activator. Although it is generally assumed that these mixtures will lead to transalkylation and the formation of zirconium isobutyl species, the precise chemistry of these mixtures under catalytic conditions is so far unknown. Zirconocene methyl derivatives are commonly used as precursors, although the methyl ligand is a poor model for a polymeryl chain insofar as it lacks steric bulk, is remarkably slow to insert alkenes, and acts readily as a bridging ligand

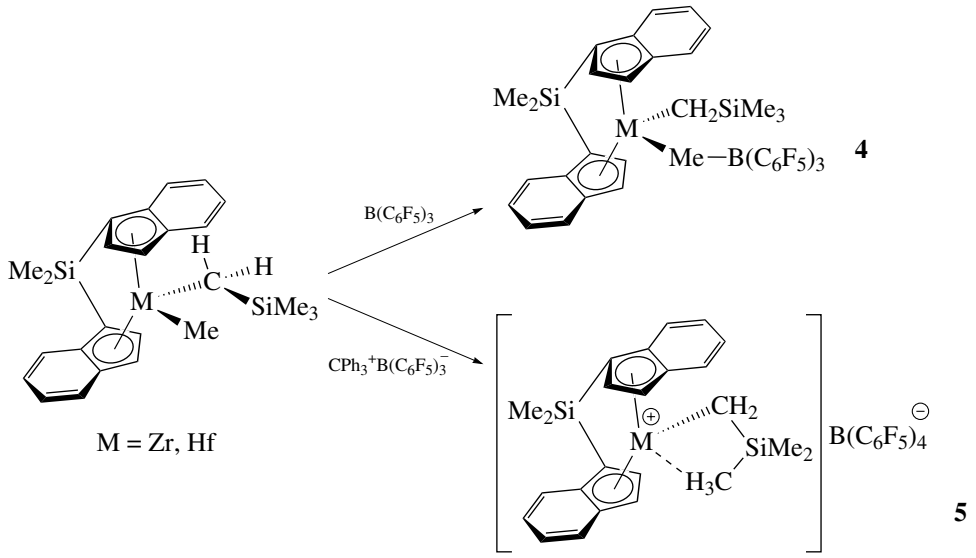

Scheme 7.

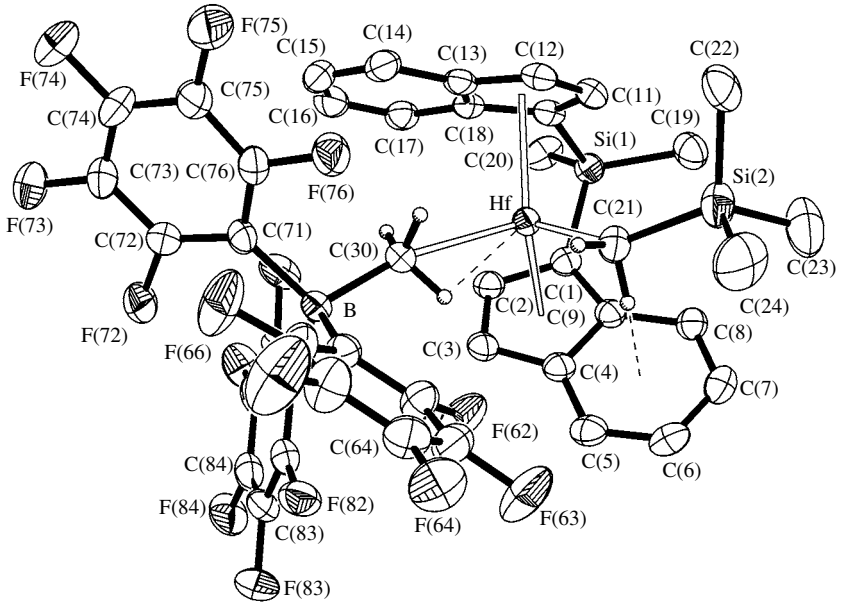

Fig. 3. Molecular structure of (SBI)Hf(CH_2SiMe_3)(μ-Me)$B(C_6F_5)_3$. Ellipsoids are drawn at a 50% probability level.

whereas higher alkyls do not. We wished therefore to use a more realistic catalyst model. Since neopentyl ligands are known to undergo β-methyl abstraction and eliminate isobutene [57], we chose to prepare zirconocene trimethylsilylmethyl derivatives, Scheme 7 [48].

The readily accessible mixed-alkyl metallocene complexes (SBI)M(Me)CH_2SiMe_3 (M = Zr, Hf) provide a route for zwitterions (SBI)M(CH_2SiMe_3)(μ-Me)$B(C_6F_5)_3$. The crystal structure of this compound confirmed the familiar methyl-bridged structure (Fig. 3) [58].

Ion pairs of 14-electron alkyl complexes $[(SBI)MCH_2SiMe_3^+\cdots B(C_6F_5)_4^-]$ could not be crystallized but turned out to be of remarkable thermal stability, and in toluene solution at room temperature they showed no deterioration over a period of several days. The β-methyl branched alkyl ligand acts as a model for ligated polypropylene. The variable-temperature NMR spectra confirm that here agostic bonding to β-methyl substituents is preferred over anion coordination, resulting in an outer-sphere ion pair structure. There are, therefore, significant differences in the structures

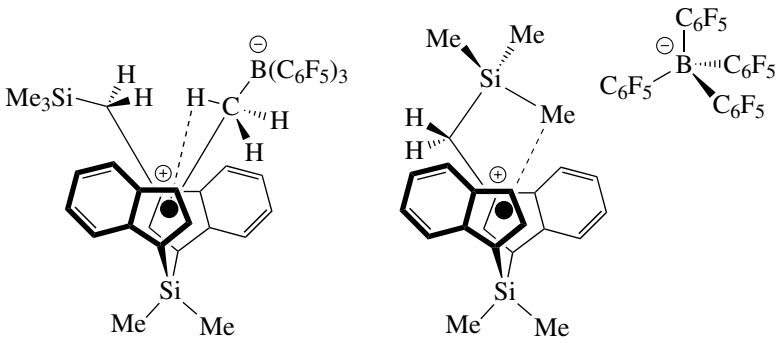

Fig. 4. Structures of inner-sphere and outer sphere M–CH_2SiMe_3 ion pairs.

of $MeB(C_6F_5)_3^-$ and $B(C_6F_5)_4^-$ complexes: the inner- vs. outer-sphere ion pairs and outwards vs. inwards pointing conformations of the alkyl ligand (Fig. 4) [58].

These complexes provide useful information about the ion pair dynamics and solution structures. Site epimerization is faster than with $Zr–CH_3$ analogues. Rates decrease with decreasing metallocene concentration; the observed values therefore represent upper limits for the exchange rates expected for the low metal concentrations employed under catalytic conditions. The data also provide an interesting illustration of the stereochemistry of chain swinging. Thus, while the bridge–$SiMe_2$ signals show a typical pattern for the two-site exchange expected for this symmetrization process, the $Zr–CH_2$ signals remain unaffected and appear as an AB pattern throughout the observed temperature range; that is, the methylene hydrogens H^a and H^b do not interchange. This behavior is consistent with a chain swinging mechanism that involves a 180° rotation of the alkyl ligand (Scheme 8), as is indeed required by the symmetry in a system with a C_2-symmetric ligand framework.

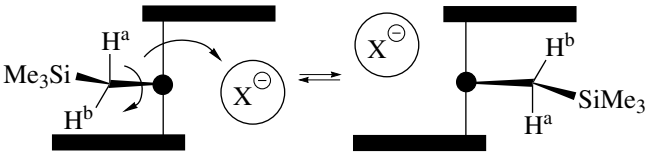

Scheme 8.

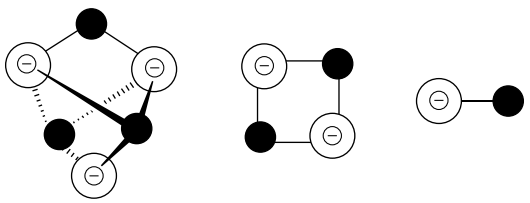

Scheme 9.

Pulsed field-gradient spin echo (PGSE) and nuclear Overhauser effect (NOE) NMR experiments showed the influence of bulky alkyl chains on the solution structures of $(SBI)Zr(CH_2SiMe_3)(\mu\text{-}Me)B(C_6F_5)_3$ and $[(SBI)ZrCH_2SiMe_3^+ \cdots B(C_6F_5)_4^-]$. As expected, the $MeB(C_6F_5)_3$ compound in toluene-d_8/1,2-difluorobenzene 9 : 1 exists as a simple inner-sphere ion-pair (ISIP). ^{19}F, ^1H HOESY NMR investigations showed that the anion binds to the cation in the usual fashion with the B–Me vector pointing toward the Zr centre. In agreement with this structure, only the *o*-F fluorine nuclei interact with the CH_2SiMe_3 signal and with the CH_2SiMe_3 resonance, while both the *m*-F and *p*-F nuclei give a weak interaction with the CH_2SiMe_3 signal. From these observations, we conclude that the CH_2SiMe_3 ligand is preferentially oriented in such a way that the bulky $SiMe_3$ group is pointing away from the anion, as shown in the crystal structure.

By contrast, $[(SBI)ZrCH_2SiMe_3^+ \cdots B(C_6F_5)_4^-]$ in toluene-d_8/1,2-difluorobenzene 9 : 1 at higher concentrations (10 mM) forms mainly ion hextuples (aggregation number N = 3.12), indicative of the more ionic character of an outer-sphere ion pair (OSIP). This is a consequence of the relegation of the anion into the second coordination sphere caused by the γ-agostic interaction. At lower [Zr] and lower temperature, ion quadruples predominate. It is possible that further dilution may lead to simple ion pairs, although these were not observed (Scheme 9).

Mechanistic models. The mechanism of 1-alkene polymerization with such ion pair catalysts has recently been a matter of debate in the literature. Early kinetic studies by Fink on titanocene-catalyzed ethylene oligomerizations have led to a model in which the catalyst precursor is activated by some chemical process (such as anion displacement) to give an active species that is not spectroscopically detectable, and each monomer insertion can be followed by the (reversible) stabilization of the product as a dormant state, in a model termed "intermittent mechanism" [59–63]. More recently, Brintzinger et al. studied the reaction of a

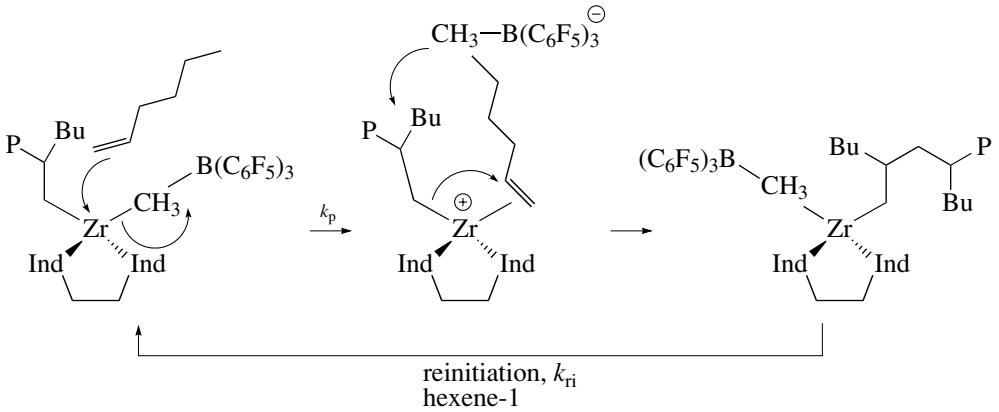

Scheme 10.

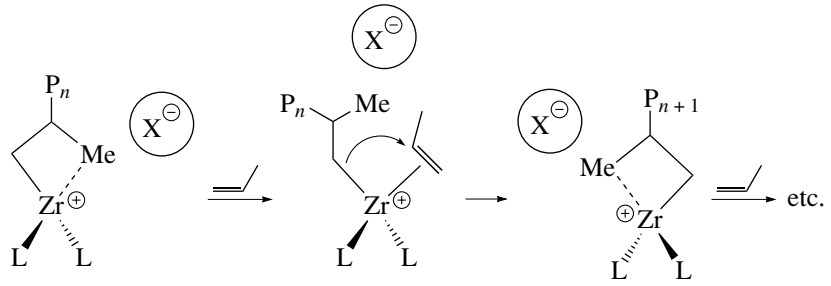

Scheme 11.

series of zirconocene methylborates with di-*n*-butyl ether (DBE) as an "alkene surrogate." Here, anion displacement was slow, and the authors suggested that these findings pointed towards a mechanism in which chain growth was initiated by anion displacement and proceeded by successive rapid monomer enchainments, which were interrupted by slow anion re-coordination [64]. On the other hand, Landis showed that in hexene-1 polymerizations with (EBI)$ZrMe_2$/$B(C_6F_5)_3$ at low temperature, where the system is living and Zr-polymeryl species are directly NMR-observable, each monomer insertion was followed by anion reassociation in a concerted anion displacement—monomer insertion—anion reassociation reaction sequence, a process termed the "continuous" propagation mode ($k_p = k_{ri}$, Scheme 10) [65].

Clearly the very high activities observed with OSIP-type $B(C_6F_5)_4^-$ based catalysts and the low contributions of the anion to the activation barrier are not consistent with a mechanism in which the anion recoordinates and forms a tight ion pair with the metal centre after each insertion step. The sequence in this case is probably better depicted in Scheme 11. Here there is no anion coordination; the anion is, however, kept within the solvent cage (in low polarity media there is no free ion diffusion). Each insertion step involves an increase in the cation–anion distance, which explains the contributions of the counter anion to the activation barrier, followed by alkyl/anion site exchange, as required within a catalytic cycle, since the structure of the product must correspond to the starting point of the insertion event. In this respect, the "continuous" ISIP mechanism and the OSIP reaction sequence are similar in principle: both follow an associative interchange (I_a) pathway. The site exchange of the (very large) anion is probably best understood as a rotation of the metallocenium cation with respect to the anion.

CONCLUSIONS

In summary, we have shown methods for the quantification of catalyst activity in high-activity metallocene systems and have demonstrated, in particular, the contribution the counter anion makes to catalyst activity, the structure of the active species, ion aggregation, and the dynamics of well-defined ion pairs. The synthesis of zirconocene trimethylsilylmethyl complexes in particular has provided insight into the stereochemistry of site epimerization and the mechanism of chain propagation and has highlighted important differences in the structure and ligand conformation of ISIP $MeB(C_6F_5)_3^-$ and OSIP $B(C_6F_5)_4^-$ ion pairs. Both agostic interactions of β-methyl branched alkyl ligands and *sec*-alkyl species are likely to be resting states in these

catalysts, at least with the SBI ligand system investigated here. If one accepts the definitions of "active species" and "dormant states" employed here, the chain propagation sequence is in agreement with an "intermittent" model along the lines of an associative interchange mechanism.

ACKNOWLEDGMENTS

This work was supported by the British Engineering and Physical Sciences Research Council. We are grateful to Prof. A. Macchioni (University of Perugia, Italy) for PGSE and NOE NMR measurements and helpful discussions.

REFERENCES

1. Bochmann, M., *J. Organomet. Chem.*, 2004, vol. 689, p. 3982.
2. Chen, E.Y.X. and Marks, T.J., *Chem. Rev.*, 2000, vol. 100, p. 1391.
3. Bochmann, M., *J. Chem. Soc., Dalton Trans.*, 1996, p. 255.
4. Brintzinger, H.H., Fischer, D., Mülhaupt, R., Rieger, B., and Waymouth, R., *Angew. Chem., Int. Ed. Engl.*, 1995, vol. 34, p. 1143.
5. Bochmann, M., in *Catalytic Mechanisms from Spectroscopic Measurements*, Heaton, B.T., Ed., Weinheim: Wiley–VCH, 2005, p. 311.
6. Lupinetti, A.J. and Strauss, S.H., *Chemtracts—Inorg. Chem.*, 1998, vol. 11, p. 565.
7. Strauss, S.H., *Chem. Rev.*, 1993, vol. 93, p. 927.
8. Bochmann, M. and Jaggar, A.J., *J. Organomet. Chem.*, 1992, vol. 424.
9. Bochmann, M., *Angew. Chem., Int. Ed. Engl.*, 1992, vol. 31, p. 1181.
10. Yang, X., Stern, C.L., and Marks, T.J., *Organometallics*, 1991, vol. 10, p. 840.
11. Siedle, A.R., Lamanna, W.M., Newmark, R.A., Stevens, J., Richardson, D.E., and Ryan, M., *Makromol. Chem., Macromol. Symp.*, 1993, vol. 66, p. 215.
12. Chien, J.C.W., Song, W., and Rausch, M.D., *J. Polym. Sci., Part A: Polym. Chem.*, 1994, vol. 32, p. 2387.
13. Eur. Pat. Appl. EP 277 004, 1988.
14. Eur. Pat. Appl. EP 426 637, 1990.
15. Eur. Pat. Appl. EP 427 697, 1991.
16. Yang, X., Stern, C.L., and Marks, T.J., *J. Am. Chem. Soc.*, 1991, vol. 113, p. 3623.
17. Ewen, J.A. and Elder, M.J., *Makromol. Chem., Macromol. Symp.*, 1993, vol. 66, p. 179.
18. Ewen, J.A., *Stud. Surf. Sci. Catal.*, 1994, vol. 89, p. 405.
19. Jia, L., Yang, X., Ishihara, A., and Marks, T.J., *Organometallics*, 1995, vol. 14, p. 3135.
20. Chen, Y.X., Stern, C.L., Yang, S., and Marks, T.J., *J. Am. Chem. Soc.*, 1996, vol. 118, p. 12451.
21. Jia, L., Yang, X., Stern, C.L., and Marks, T.J., *Organometallics*, 1997, vol. 16, p. 842.
22. Chen, Y.X. and Marks, T.J., *Organometallics*, 1997, vol. 16, p. 3649.
23. Chen, Y.X., Stern, C.L., and Marks, T.J., *J. Am. Chem. Soc.*, 1997, vol. 119, p. 2582.
24. Chen, Y.X., Metz, M.V., Li, L., Stern, C.L., and Marks, T.J., *J. Am. Chem. Soc.*, 1998, vol. 120, p. 6287.
25. Li, L. and Marks, T.J., *Organometallics*, 1998, vol. 17, p. 3996.
26. Metz, M.V., Schwartz, D.J., Stern, C.L., Nickias, P.N., and Marks, T.J., *Angew. Chem., Int. Ed. Engl*., 2000, vol. 39, p. 1312.
27. Sun, Y., Metz, M.V., Stern, C.L., and Marks, T.J., *Organometallics*, 2000, vol. 19, p. 1625.
28. Metz, M.V., Sun, Y., Stern, C.L., and Marks, T.J., *Organometallics*, 2002, vol. 21, p. 3691.
29. Chen, M.C. and Marks, T.J., *J. Am. Chem. Soc.*, 2001, vol. 123, p. 11803.
30. Abramo, G.P., Li, L., and Marks, T.J., *J. Am. Chem. Soc.*, 2002, vol. 124, p. 13966.
31. Wang, J., Li, H., Go, N., Li, L., Stern, C.L., and Marks, T.J., *Organometallics*, 2004, vol. 23, p. 5112.
32. Li, H., Li, L., and Marks, T.J., *Angew. Chem., Int. Ed. Engl.*, 2004, vol. 43, p. 4937.
33. Chen, E.Y.X., Kruper, W.J., Roof, G., and Wilson, D.R., *J. Am. Chem. Soc.*, 2001, vol. 123, p. 745.
34. Köhler, K. and Piers, W.E., *Can. J. Chem.*, 1998, vol. 76, p. 1249.
35. Köhler, K., Piers, W.E., Jarvis, A.P., Xin, S., Feng, Y., Brasakis, A.M., Collins, S., Clegg, W., Yap, G.P.A., and Marder, T.B., *Organometallics*, 1998, vol. 17, p. 3557.
36. Williams, V.C., Piers, W.E., Clegg, W., Elsegood, M.R.J., Collins, S., and Marder, T.B., *J. Am. Chem. Soc.*, 1999, vol. 121, p. 3244.
37. Williams, V.C., Dai, C., Li, Z., Collins, S., Piers, W.E., Clegg, W., Elsegood, M.R.J., and Marder, T.B., *Angew. Chem., Int. Ed. Engl.*, 1999, vol. 38, p. 3695.
38. Williams, V.C., Irvine, G.J., Piers, W.E., Li, Z., Collins, S., Clegg, W., Elsegood, M.R.J., and Marder, T.B., *Organometallics*, 2000, vol. 19, p. 1619.
39. Lancaster, S.J., Walker, D.A., Thornton-Pett, M., and Bochmann, M., *Chem. Commun.*, 1999, p. 1533.
40. Patent WO 99/42467, 1999.
41. Zhou, J., Lancaster, S.J., Walker, D.A., Beck, S., Thornton-Pett, M., and Bochmann, M., *J. Am. Chem. Soc.*, 2001, vol. 123, p. 223.
42. Lancaster, S.J., Rodriguez, A., Lara-Sanchez, A., Hannant, M.D., Walker, D.A., Hughes, D.L., and Bochmann, M., *Organometallics*, 2002, vol. 21, p. 451.
43. Hannant, M.D., Schormann, M., Hughes, D.L., and Bochmann, M., *Inorg. Chim. Acta*, 2005, vol. 358, p. 1683.
44. Möhring, P.C. and Coville, N.J., *J. Organomet. Chem.*, 1994, vol. 479, p. 1.
45. Song, F., Cannon, R.D., and Bochmann, M., *J. Am. Chem. Soc.*, 2003, vol. 125, p. 7641.
46. Bochmann, M., Song, F., Rodriguez, A., and Cannon, R.D., *PMSE Preprints*, 2002, vol. 87, p. 36.
47. Song, F., Hannant, M.D., Cannon, R.D., and Bochmann, M., *Macromol. Symp.*, 2004, vol. 213, p. 173.
48. Song, F., Cannon, R.D., and Bochmann, M., *Chem. Commun.*, 2004, p. 542.

49. Song, F., Cannon, R.D., Lancaster, S.J., and Bochmann, M., *J. Mol. Catal.*, 2004, vol. 218, p. 21.
50. Busico, V., Cipullo, R., and Esposito, V., *Macromol. Rapid Commun.*, 1999, vol. 20, p. 116.
51. Liu, Z., Somsook, E., and Landis, C.R., *J. Am. Chem. Soc.*, 2001, vol. 123, p. 2915.
52. Liu, Z., Somsook, E., White, C.B., Rosaaen, K.A., and Landis, C.R., *J. Am. Chem. Soc.*, 2001, vol. 123, p. 11193.
53. Resconi, L., Cavallo, L., Fait, A., and Piemontesi, F., *Chem. Rev.*, 2000, vol. 100, p. 1253.
54. Busico, V. and Cipullo, R., *Prog. Polym. Sci.*, 2001, vol. 26, p. 443.
55. Landis, C.R., Sillars, D.R., and Batterton, J.M., *J. Am. Chem. Soc.*, 2004, vol. 126, p. 8890.
56. Busico, V., Cipullo, R., Romanelli, V., Ronca, S., and Togrou, M., *J. Am. Chem. Soc.*, 2005, vol. 127, p. 1608.
57. Horton, A.D., *Organometallics*, 1996, vol. 15, p. 2675.
58. Song, F., Cannon, R.D., Lancaster, S.J., Schormann, M., Humphrey, S.M., Zuccaccia, C., Macchioni, A., and Bochmann, M., *Organometallics*, 2005, vol. 24, p. 1315.
59. Schnell, D. and Fink, G., *Angew. Macromol. Chem.*, 1974, vol. 39, p. 131.
60. Fink, G. and Zöller, W., *Makromol. Chem.*, 1981, vol. 182, p. 3265.
61. Fink, G. and Schnell, D., *Angew. Macromol. Chem.*, 1982, vol. 105, p. 31.
62. Mynott, R., Fink, G., and Fenzl, W., *Angew. Macromol. Chem.*, 1987, vol. 154, p. 1.
63. Fink, G., Fenzl, W., and Mynott, R.Z., *Z. Naturforsch., B: Chem. Sci.*, 1985, vol. 40, p. 158.
64. Schaper, F., Geyer, A., and Brintzinger, H.H., *Organometallics*, 2002, vol. 21, p. 473.
65. Landis, C.R., Rosaeen, K.A., and Sillars, D.R., *J. Am. Chem. Soc.*, 2003, vol. 125, p. 1710.